7th International Conference on Silicon Photovoltaics, SiliconPV 2017

Comparison of iron-related recombination centers in boron, gallium, and indium doped silicon analyzed by defect parameter contour mapping

Tine U. Nærland[a],*, Simone Bernardini[a], Nathan Stoddard[b], Ethan Good[c], André Augusto[d] and Mariana Bertoni[a]

[a]Ira A. Fulton Schools of Engineering, Arizona State University, 650 E. Tyler Mall, Tempe, AZ 85287, USA
[b]Solar World Industries America, 25300 NW Evergreen Rd Hillsboro, OR 97124, USA
[c]SunEdison, 7832 N Leadbetter Rd, Portland, OR 97203, USA
[d]Solar Power Lab, Arizona State University Research Park, 7700 South River Parkway, Tempe, AZ 85284, USA

Abstract

In this work, we are showing that iron (Fe) related defects in mono-silicon have very different recombination characteristics depending on the doping element employed. While the defect characteristics of the Fe in its dissociated state is comparably the same in the materials of investigation, the defect characteristics of the associated state vary considerably. By using, defect parameter contour mapping (DPCM), a newly developed method for analyzing temperature and injection dependent lifetime data, we have for the first time, been able to show that in the case of gallium doping it is the orthorhombic state of the Fe-acceptor complex that is dominating the lifetime.

Keywords: Fe-contamination; Boron-doping; Gallium-doping; Indium-doping; Lifetime Spectroscopy; DPCM

1. Introduction

It is well known that replacing boron (B) with gallium (Ga) as a p-type dopant in silicon (Si) suppresses the light-induced degradation (LID) originated by B-O related defects [1]. Indium (In) doped Si was for a long time believed to have the same un-degrading behavior as Ga-Si but was recently reported to have a similarly degrading behavior as B-doped silicon [2]. Ga nor In are, however, commonly used as a dopant in crystalline Si solar cells due to their low segregation coefficient, which causes large resistivity variations in the silicon ingot after solidification. Lately,

however, new methods for overcoming this problem have been developed, enabling low resistivity variation over the crystal height. It has been shown that Ga-doped and In-doped Si wafers exhibit very high minority carrier lifetimes (MCL) [3],[4]. A shift to Ga-Si that does not degrade with light, in existing p-type processing lines could, therefore, have a massive impact on the levelized cost of electricity. Iron contamination in p-type silicon has, for a long time, been known to be severe to electronic performance [5]. In contrast to LID, however, iron is known to reduce the minority carrier lifetime irrespective of the doping agent. There has, however, been few studies on the extent of the problem with iron contamination in Ga-Si or In-Si [6] and in this paper, we intend to give more insight into this topic.

In crystalline p-type silicon, we know that highly mobile Fe atoms are forming electrically active pairs with shallow substitutional acceptors (A_s) such as boron, aluminum, gallium, and indium [5]. The chemical reaction for the dissociation/association process is:

$$Fe_i^+ + A_s^- = FeA_s \qquad (1)$$

By optical, thermal or electronic stimulation the pairs will dissociate into their individual constituents. The two different states of Fe have markedly different injection dependence of the minority carrier lifetime, enabling investigation of these defects by lifetime spectroscopy. In the following, we are comparing the defect energies (E_t) and the capture cross section ratios (k) for the Fe_i^+ and the FeA_s defects in B-Si, Ga-Si and In-Si respectively.

Nomenclature

ARV   Average Residual Value
DPCM   Defect Parameter Contour Mapping
IDLS   Injection Dependent Lifetime Spectroscopy
LID   Light Induced Degradation
TIDLS Temperature and Injection Dependent Lifetime Spectroscopy
E_t Energy Level of Defect
k Capture Cross Section Ratio

---

2. Experimental and analysis

In the study we investigated three types of mono-silicon material: B-doped silicon ($N_B = 9.9 \times 10^{15}$ cm^{-3}), Ga-doped silicon ($N_{Ga} = 1.2 \times 10^{16}$ cm^{-3}), and In-doped silicon ($N_{In} = 7.6 \times 10^{15}$ cm^{-3}). Two sets of samples were prepared for each doping type; one set to be intentionally contaminated with Fe and one set to serve as a reference. The intentionally Fe-contaminated wafers were first annealed at 400°C on an iron covered hotplate for 1h with a subsequent 1h annealing in a muffle furnace at 800°C to ensure uniform Fe distribution throughout the wafer thickness. Prior to lifetime measurements, the wafers were etched, cleaned, textured, and thereafter subjected to a 50 nm double side passivation by plasma-enhanced chemical-vapor-deposited (PECVD) hydrogenated amorphous silicon (a-Si:H). To measure the temperature and injection level-dependent effective carrier lifetimes, a contactless quasi-steady-state photoconductance QSSPC technique was applied.

In this work, we have used our recently developed defect parameter contour mapping (DPCM) method to determine the difference in recombination behavior of intentionally Fe-contaminated B, Ga, and In-doped wafers. The method is a novel and comprehensive way of analyzing temperature and injection dependent lifetime spectroscopy (TIDLS) data that enables direct comparison of the defect energies (E_t) and capture cross section ratios (k) associated with the Fe-related defects in these materials. A detailed description of this method can be found in [7].

3. Results and discussion

Both B and In-doped Cz-Si and mc-Si suffer from LID under carrier injection [2],[8]. In Fig. 1 we have used uncontaminated wafers to investigate the lifetime degradation with light ourselves. As shown in Fig. 1 the Ga-Si is the only of the three materials used for this investigation not prone to carrier induced degradation.
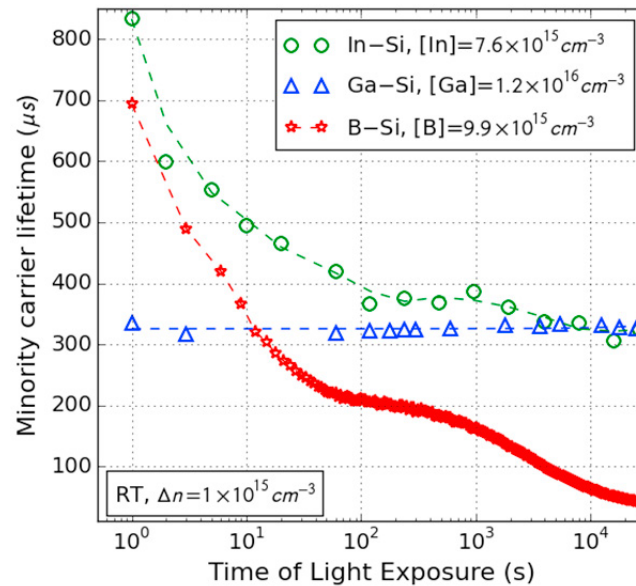

Fig. 1 Response in minority carrier lifetime to light soaking for as-grown B-doped, Ga-doped and In-doped wafers. The lifetime of the B-doped and In-doped wafers are severely reduced by light exposure, whereas the lifetime of the Ga-doped silicon remains constant. The data is collected as described in ref. [9].

Setting light induced degradation to the side, we want to look at the characteristics of the defects that these three doping elements produce in combination with Fe. The results might give useful information on the differences in operating mechanisms of these three acceptors alongside with a basis for determining the severity of iron contamination taking into account doping element and iron concentration. As mentioned introductorily shallow acceptors like B, Ga and In will form electrically active complexes with Fe, through electrostatic attraction [10]. The complexes can be split by applying heat or light and the minority carrier lifetime will then be dominated by the interstitial Fe atom left behind by the acceptor. In Fig. 2 we show lifetime curves measured on iron contaminated B-doped, Ga-doped, and In-doped Si before and after light soaking at room temperature and it can be observed that the before and after light curves for each of the doping-types is crossing at a certain injection level. (For the In-doped wafer the crossover is not perceptible due to lack of data in the relevant injection range, but it is reasonable to believe that the two curves will cross at a lower injection.) The point where the curves are crossing is commonly referred to as the crossover point [11] and is a characteristic for Si-containing iron-acceptor defects. The values of lifetime can be cycled back and forth with exposure to light and storage in dark.
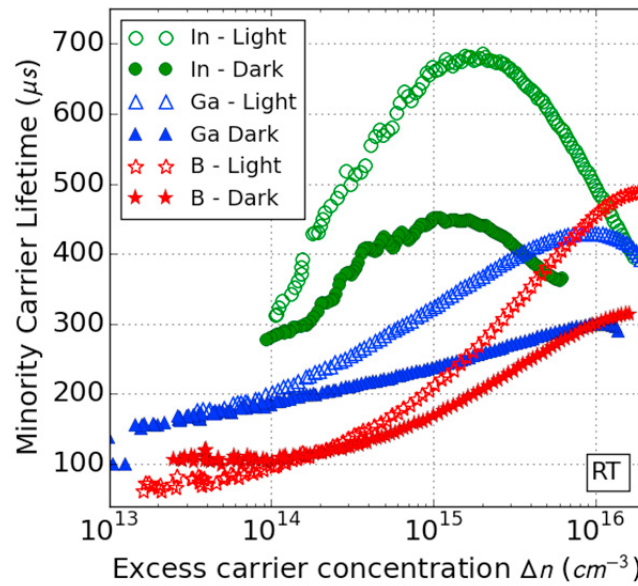
Fig. 2 Lifetime curves for B, Ga and In-doped wafers measured after; wafers had been stored in the dark for 1 week and after light soaking for 10 min.

The lifetime curves presented in Fig. 2 are measured at room temperature. In Injection Dependent Lifetime Spectroscopy (IDLS), lifetime curves like these, measured at room temperature, would be attempted fitted to Shockley-Read-Hall (SRH) theory to extract information on the defect energy level in the band gap (E_t) and possibly the electron and hole capture cross section ratio (k) [12]. To reveal significantly more definite information on the E_t and k value, lifetime curves like these can be measured at different temperatures; a technique commonly referred to as Temperature and Injection Dependent Lifetime Spectroscopy (TIDLS). To take full advantage of the information concealed in the TIDLS data, we are using our recently introduced DPCM method (Defect Parameter Contour Mapping) [7] to extract the E_t and k values of the defects. The method takes advantage of substantial computing power and is based on using SRH theory to calculate the fit quality of a simulated curve to a measured curve, for a given range of values E_t and the capture cross-section ratio (k). For every $E_t – k$ combination the time constants τ_{p0} and τ_{n0} are varied until the best fit of the experimental data is obtained. The quality of the fit, represented by lighter color in the contour plot, is determined by calculating an *Average Residual Value* (ARV):

$$Average\ Residual\ Value = \sum_{j=1}^{m}\left(\left(\sum_{i=1}^{n}\frac{|\tau_{measured,i,j} - \tau_{model,i,j}|}{\tau_{measured,i,j}}\right)/n\right)/m \qquad (1)$$

where n is the number of injection level values and m is the number of temperatures taken into account. Three significant advantages of using DPCM to determine electronic properties of defects are that (i) the method does not rely on highly uncertain estimations of the contaminant concentration from diffusion calculations, (ii) that we do not simplify the SRH-equation for high or low injection range conditions with the uncertainty that this introduces, and (iii) that the whole E_t and k space is projected, preventing us from overlooking other E_t and k combinations generating good fits. A more detailed description of the method can be found in ref. [7].

In Fig. 3 the DPCM maps for the three dopants in dark and light, respectively, are given. The maps are made from TIDLS data obtained with a Sinton Lifetime tester with an integrated temperature stage. The maps are showing similar best fit ARV's, establishing a good starting point for comparison. The exact values for the E_t and k values extracted from the maps are given in Table I, together with errors considering a change of 5 % (absolute) in the

ARV. It can be seen that from the dissociated state of the iron-acceptor complex in Fig. 3b, d, and f that the interstitial Fe_i defect in all cases are described by a deep-in-the-band-gap defect energy level and a k-value greater than unity. A k-value greater than unity means that the capture cross section for the electrons is greater than the capture cross section for the holes, a common characteristic of donor defects. Although there are differences in the E_t and k value of the Fe_i for the different doping elements in this study, they are, except for the In-Si k-value, all in line with former research on E_t and k values for Fe_i ranging from $E_t = E_V + (0.38 - 0.48)$ to $k = 51 – 571$ [5], [13],[14]. The reason for the differing k value for the In-Si is something that we are currently investigating and will be addressed in a future publication.
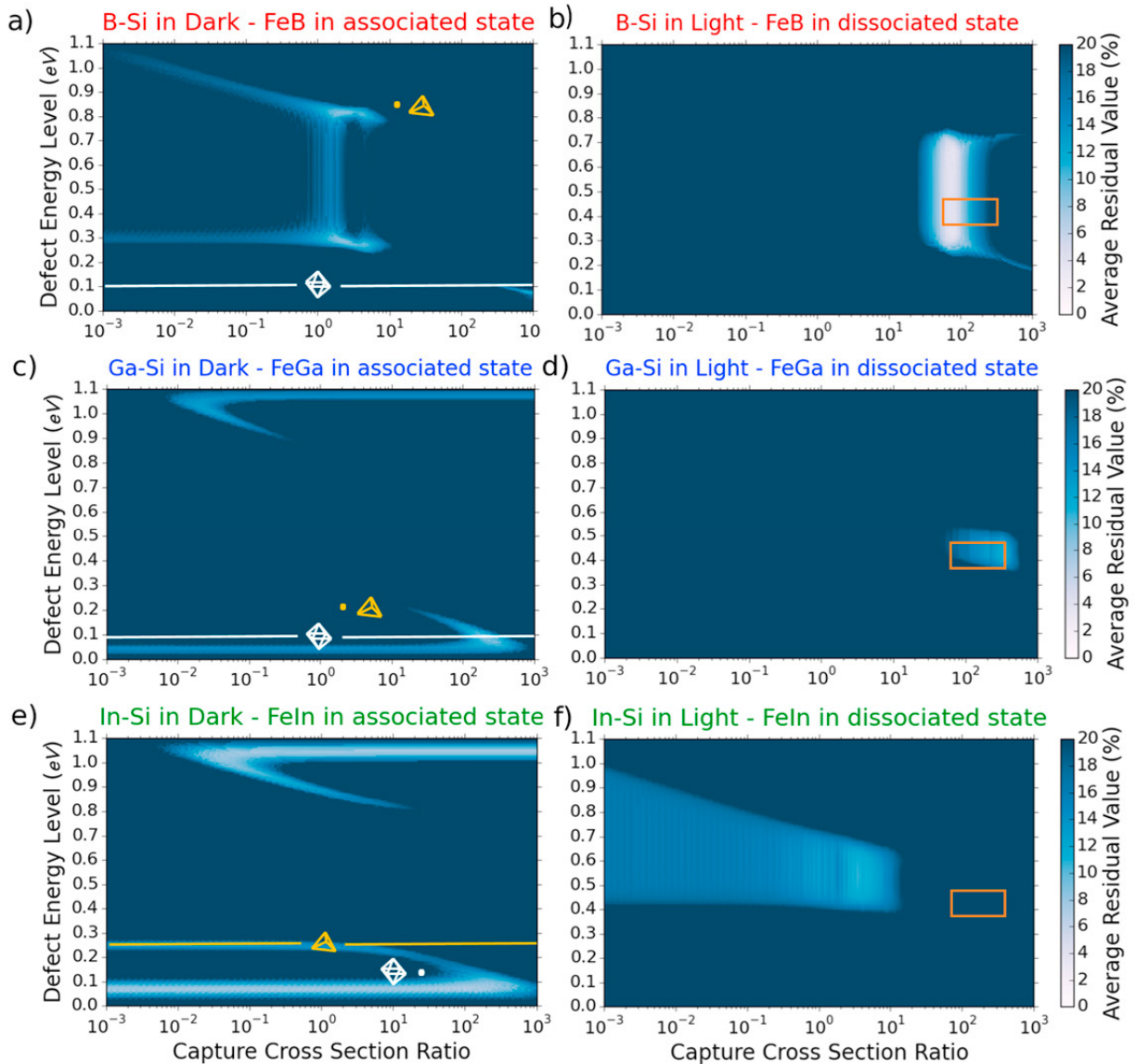

Fig. 3 TIDLS-DPCM plots of Fe-contaminated B-Si, Ga-Si and In-Si in the associated state (a), (c) and (e) and the dissociated state (b), (d) and (f). In (b), (d) and (f) the orange box indicates the range of parameters found in literature for the Fe_i defect. In (a), (c) and (e) the yellow trigonal pyramid indicates literature values on the trigonal configuration of the FeAs complex. The white orthorhombic "diamond" indicates literature values for the orthorhombic configuration of the FeAs complex. The line in relation to the configuration is indicating that the k-value has not been reported yet. In the associated state, the temperature range of the analyzed lifetime curves is 21˚C - 221˚C. In the dissociated state the temperature range of the analyzed lifetime curves is 21˚C - 121˚C The τ_{p0} range used for the SRH-fitting in these plots is ~ 10^{-11} - 10^{-2} s.

Table 1 Average Residual Value (ARV), Energy levels (E_t) and capture cross section ratios (k) with upper and lower error-levels for iron-related recombination centers in crystalline silicon determined in this study.

	ARV (%)	E_t	k	$E_{t,min}$	$E_{t,max}$	k_{min}	k_{max}
				Error accounting for +5 % ARV			
FeB	8.40	E_C - 0.31	2.4	E_C - 0.28	E_C - 0.35	0.84	5.9
Fe_i (B-Si)	8.3	E_V + 0.39	74	E_V + 0.27	E_V + 0.72	47	115
FeGa	8.6	E_V + 0.09	232	E_V + 0.04	E_V + 0.14	71	499
Fe_i (Ga-Si)	11.4	E_V + 0.43	329	E_V + 0.37	E_V + 0.51	116	466
FeIn	6.9	E_V + 0.08	116	E_V + 0.04	E_V + 0.12	0.001	659
Fe_i (In-Si)	10.8	E_V + 0.54	3.4	E_V + 0.41	E_V + 0.72	0.05	10

Studies with measurements of electron spin resonance (ESR) have clarified that Fe-acceptor pairs in their associated state have two structural configurations: trigonal and orthorhombic symmetry [15], [16], [17]. The pairs with trigonal symmetry have Fe atoms occupying the first nearest-neighbor interstitial sites adjacent to acceptors along the <111> direction. The pairs with orthorhombic symmetry have Fe atoms that occupy the second nearest-neighbour interstitial sites adjacent to acceptors along the <100> direction [17],[18],[19]. See Fig. 4. Both of these configurational pairs are observed experimentally in Fe-contaminated specimens in the cases of B-, Al-, Ga-, and In-doped samples but with some variations. For example, the orthorhombic FeB pair is only detected when the sample is illuminated or injected with minority carriers at temperatures below 150K [20], and so in FeB-materials, the only configuration that can be seen at room temperature is the trigonal configuration. In Fig. 3a the DPCM plot of B-Si in the associated FeB state shows two regions of good fit: one in the upper bandgap half and one in the lower band gap half. The two regions are due to carrier recombination symmetry over the bandgap which is inevitable in lifetime spectroscopy. It is, however, commonly accepted that the acceptor level in the upper band gap half at $E_t \approx E_C$ - 0.27 is the true recombination active defect center for the trigonal configuration of FeB [21].
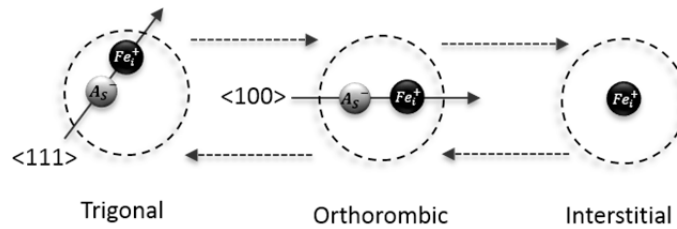

Fig. 4. The three states schematically shown in this figure are the states in which the iron-acceptor will occur in silicon doped with boron, gallium, aluminium, and indium. The state will change upon illumination, heating or carrier injection [18]

As pointed out by Zhao *et al.*[22], there is an overall trend that when shifting to an acceptor with a higher atomic number, the stability of iron-acceptor pairs changes from the trigonal configuration to the orthorhombic. In In-Si material it is i.e. found that it is the orthorhombic configuration that is stable at room temperature [23].

Theoretical calculations show, however, that as for FeB the trigonal configuration of the FeGa is predominant at room temperature [22]. Comparing Fig. 3 a), c) and e) it is obvious that the characteristics of the defect center dominating in the associated state of B-Si and Ga-Si and In-Si samples are very different. In Ga-Si and In-Si two defect centers associated with the associated state has been observed by ERS: a trigonal donor level at $E_t = E_V$ + 0.21 eV and an orthorhombic donor level at $E_t = E_V$ + 0.10 eV has been seen in the Ga-Si [24], and a trigonal donor level of $E_t = E_V$ + 0.27 eV and an orthorhombic donor level at $E_t = E_V$ + 0.15 eV has been seen in the In-Si [5]. From Fig. 3c and d it is observable that in the TIDLS analysis reported in here, it is the "shallower" orthorhombic defect centers that act as the main recombination center in the cases of FeIn and FeGa as opposed to in Fig. 3a, in the case of FeB, where it is the deeper trigonal center that dominates.

It has earlier been reported that the FeGa-pairs are significantly more recombination active than the FeB-pairs [6]. In this work, however - taking into account that it is the orthorhombic configuration of the FeGa complex that dominates at room temperature – we calculate that compared to B-Si with comparable doping concentration and Fe contamination, the lifetime of Ga-Si is more than doubled of B-Si. For this calculation, we have used E_t and capture cross section values reported for FeB and FeGa in ref. [6] and ref. [25] respectively.

4. Conclusion

The work presented herein is based on TIDLS analysis of Fe-containing B, Ga, and In-doped Si making no assumption regarding the configurational nature of the defects - both the trigonal and orthorhombic defect center can occur simultaneously. We observe that there is a predominance of the orthorhombic center in Ga and In-Si. This indicates that the orthorhombic defect configuration is the most stable configuration in Fe-containing Ga and In-Si at room temperature as opposed to the trigonal defect configuration as in Fe-containing B-Si.

Acknowledgement

References

[1] Sheoran M, Upadhyaya A and Rohatgi A, A Comparison of Bulk Lifetime, Efficiency, and Light-Induced Degradation in Boron- and Gallium-Doped Cast mc-Si Solar Cells, IEEE Transactions On Electron Devices, 2006;53:2764-2772.
[2] Möller C and Lauer K, Light-induced degradation in indium-doped silicon, Physica Status Solidi (RRL) – Rapid Research Letters, 2013;7:461-464.
[3] Glunz SW, Köster B, Leimenstoll T, Rein S, Schäffer E, Knobloch J and Abe T, 100 cm2 solar cells on Czochralski silicon with an efficiency of 20·2%, Prog Photovoltaics Res Appl, 2000;8:237-240.
[4] Haringer S, Giannattasio A, Alt HC and Scala R, Growth and characterization of indium doped silicon single crystals at industrial scale, Japanese Journal of Applied Physics, 2016;55:031305.
[5] Istratov AA, Hieslmair H and Weber ER, Iron and its complexes in silicon, Appl. Phys. A, 1999;69:13-44.
[6] Schmidt J and Macdonald DH. Recombination activity of iron-gallium and iron-indium pairs in silicon, J. Appl. Phys. 2005;97:113712.
[7] Bernardini S, Nærland TU, Blum AL, Coletti G and Bertoni MI, Unraveling bulk defects in high-quality c-Si material via TIDLS, Prog. Photovoltaics Res. Appl, 2017;25:209-217.
[8] Lindroos J and Savin H, Review of light-induced degradation in crystalline silicon solar cells, Solar Energy Mater. Solar Cells, 2016;147:115-126.4, .
[9] Naerland TU, Haug H, Angelskar H, Sondena R, Marstein ES and Arnberg L, Studying Light-Induced Degradation by Lifetime Decay Analysis: Excellent Fit to Solution of Simple Second-Order Rate Equation, IEEE Journal Of Photovoltaics, 2013;3:1265-1270.
[10] Wünstel K and Wagner P, Interstitial iron and iron-acceptor pairs in silicon, Appl. Phys. A, 1982;27:207-212.
[11] Macdonald DH, Geerligs LJ and Azzizi A, Iron detection in crystalline silicon by carrier lifetime measurements for arbitrary injection and doping, J. Appl. Phys. 2004;95:1021-1028.
[12] Rein S, Rehrl T, Warta W and Glunz SW, Lifetime spectroscopy for defect characterization: Systematic analysis of the possibilities and restrictions, J. Appl. Phys. 2002;91:2059-2070.
[13] Macdonald D, Tan J and Trupke T, Imaging interstitial iron concentrations in boron-doped crystalline silicon using photoluminescence, J. Appl. Phys. 2008;103:073710.
[14] Rein S and Glunz SW. Electronic properties of interstitial iron and iron-boron pairs determined by means of advanced lifetime spectroscopy, J. Appl. Phys. 2005;98:113711.
[15] Woodbury HH and Ludwig GW, Spin Resonance of Transition Metals in Silicon, Phys. Rev., 1960;117:102.
[16] Ludwig GW and Woodbury HH, Electronic Structure of Transition Metal Ions in a Tetrahedral Lattice, Phys. Rev. Lett., 1960;5:98-100.
[17] Gehlhoff W, Emanuelsson P, Omling P and Grimmeiss HG, Electron paramagnetic resonance identification of the orthorhombic iron-indium pair in silicon, Phys. Rev. B, 1990;41:8560-8563.
[18] Dobaczewski L and Surma L, Iron-boron pair in silicon: Old problem anew, Acta Phys. Pol. A, 1996;90:613-622
[19] Takahashi H, Suezawa M and Sumino K, Relation between the Metastability and the Configuration of Iron-Acceptor Pairs in Silicon, Jap. J. of Appl. Phys., 1997;36:6807-6813.
[20] Sakauchi S, Suezawa M, Sumino K and Nakashima H. Recombinationenhanced Fe atom jump between the first and the second neighbor site of Fe–acceptor pair in Si, J. Appl. Phys. 1996;80:6198-6203.
[21] Graff K, Metal Impurities in Silicon-Device Fabrication. Springer, 1999.

[22] Zhao S, Assali LVC, Justo JF, Gilmer GH and Kimerling LC, Iron–acceptor pairs in silicon: Structure and formation processes, J. Appl. Phys. 2001;90:2744-2754.

[23] Chantre A, Trends in the Bistable Properties of Iron-Acceptor Pairs in Silicon, Mater. Sci. Forum, 1986;387:10-12.

[24] Ciszek TF, Schwuttke GH and Yang KH, Directionally solidified solar-grade silicon using carbon crucibles, J. Cryst. Growth, 1979;46:527-533.

[25] Nærland TU, Bernardini S, Haug H, Grini S, Vines L, Stoddard N and Bertoni M, On the Recombination Centers of Iron-Gallium pairs in Ga-doped silicon, Accepted for publication in J. Appl. Phys., 2017.